Spin-State Crossover Model for the Magnetism of Iron Pnictides

Jiří Chaloupka[1,2] and Giniyat Khaliullin[1]

[1]*Max Planck Institute for Solid State Research, Heisenbergstrasse 1, D-70569 Stuttgart, Germany*
[2]*Central European Institute of Technology, Masaryk University, Kotlářská 2, 61137 Brno, Czech Republic*

(Received 18 March 2013; published 14 May 2013)

We propose a minimal model describing magnetic behavior of Fe-based superconductors. The key ingredient of the model is a dynamical mixing of quasidegenerate spin states of Fe^{2+} ion by intersite electron hoppings, resulting in an effective local spin $S_{\rm eff}$. The moments $S_{\rm eff}$ tend to form singlet pairs and may condense into a spin nematic phase due to the emergent biquadratic exchange couplings. The long-range ordered part m of $S_{\rm eff}$ varies widely, $0 \leq m \leq S_{\rm eff}$, but magnon spectra are universal and scale with $S_{\rm eff}$, resolving the puzzle of large but fluctuating Fe moments. Unusual temperature dependences of a local moment and spin susceptibility are also explained.

DOI: 10.1103/PhysRevLett.110.207205 PACS numbers: 75.10.Jm, 71.27.+a, 74.70.Xa

Since the discovery of superconductivity (SC) in doped LaFeAsO [1], a number of Fe-based SCs have been found and studied [2]. Evidence is mounting that quantum magnetism is an essential part of the physics of Fe-based SCs. However, the origin of magnetic moments and the mechanisms that suppress their long-range order (LRO) in favor of SC are still not well understood.

The magnetic behavior of Fe-based SCs is unusual. The ordered moments range from 0.1–0.4$\mu_{\rm B}$, as in spin-density wave (SDW) metals like Cr, to 1–2$\mu_{\rm B}$ typical for Mott insulators, causing debates whether the spin-Heisenberg [3–8] or fermionic-SDW pictures [9–13] are more adequate. At the same time, irrespective of the strength or very presence of LRO, the Fe-ions possess the fluctuating moments $\sim$1–2$\mu_{\rm B}$ [14,15], even in apparently ''nonmagnetic'' LiFeAs and FeSe. In fact, it was noticed early on that the Fe-moments, ''formed independently on fermiology'' [16] and ''present all the time,'' [3] are instrumental to reproduce the measured bond lengths and phonon spectra [3,16–18]. Recent experiments [19–21] observe intense high-energy spin waves that are almost independent of doping, further supporting a notion of local moments induced by Hund's coupling [22] and coexisting [23–25] with metallic bands.

While the formation of the local moments in multiorbital systems is natural, it is puzzling that these moments (residing on a simple square lattice) may remain quantum disordered in a broad phase space despite a sizable interlayer coupling; moreover, the Fe-pnictides are semimetals with strong tendency of the electron-hole pairs to form SDW state, further supporting classical LRO of the underlying moments. A fragile nature of the magnetic-LRO in Fe-pnictides thus implies the presence of a strong quantum disorder effects, not captured by *ab initio* calculations that invariably lead to magnetic order over an entire phase diagram. The ideas of domain wall motion [17] and local spin fluctuations [22] were proposed as a source of spin disorder, but no clear and tractable model of quantum magnetism in Fe-based SCs has emerged to date. Here we propose such a model.

Since Fe pnictides are distinct among the other (Mn, Co, Ni) families, their unique physics should be rooted in specific features of the Fe ion itself. In fact, Fe^{2+} is famous for its spin crossover [26]; it may adopt either of $S = 0$, 1, 2 states depending on orbital splitting, covalency, and Hund's coupling. As the ionic radius of Fe is sensitive to its spin, Fe-X bond length (X is a ligand) is also crucial. In oxides, $S = 2$ is typical and $S = 0$,1 occur at high pressures only [27]. In compounds with more covalent Fe-X bonds (X = S, As, Se), $S = 0$ is more common while $S = 1$, 2 levels are higher. The basic idea of this Letter is that when the covalency and Hund's coupling effects compete, the many-body ground state (GS) is a coherent superposition of different spin states intermixed by electron hoppings, resulting in an *average* effective spin $S_{\rm eff}$ whose length depends on pressure, etc. We explore this dynamical spin-crossover idea, and find that (i) local moment $S_{\rm eff}$ may increase with temperature explaining recent data [28], (ii) interactions between $S_{\rm eff}$ contain large biquadratic exchange, and resulting spin-nematic correlations compete with magnetic LRO, (iii) the ordered moment m varies widely, but magnon spectra are universal and scale with $S_{\rm eff}$ as observed [19,20,29], and (iv) singlet correlations among $S_{\rm eff}$ lead to the increase of the spin susceptibility with temperature [30].

The Fe ions in pnictides have a formal valence state $Fe^{2+}(d^6)$. Among its possible spin states [Fig. 1(a)], low-spin ones are expected to be favored; otherwise, the ordered moment would be too large and robust. The $S = 0$, 1 states, ''zoomed-in'' further in Fig. 1(b), are most important since they can overlap in the many-body GS by an exchange of just two electrons between ions; see Fig. 1(c). The corresponding κ process converts Fe($S = 0$)-Fe($S = 0$) pair into Fe($S = 1$)-Fe($S = 1$) singlet pair and vice versa; this requires the interorbital hopping which is perfectly allowed for $\sim$109° Fe-As-Fe

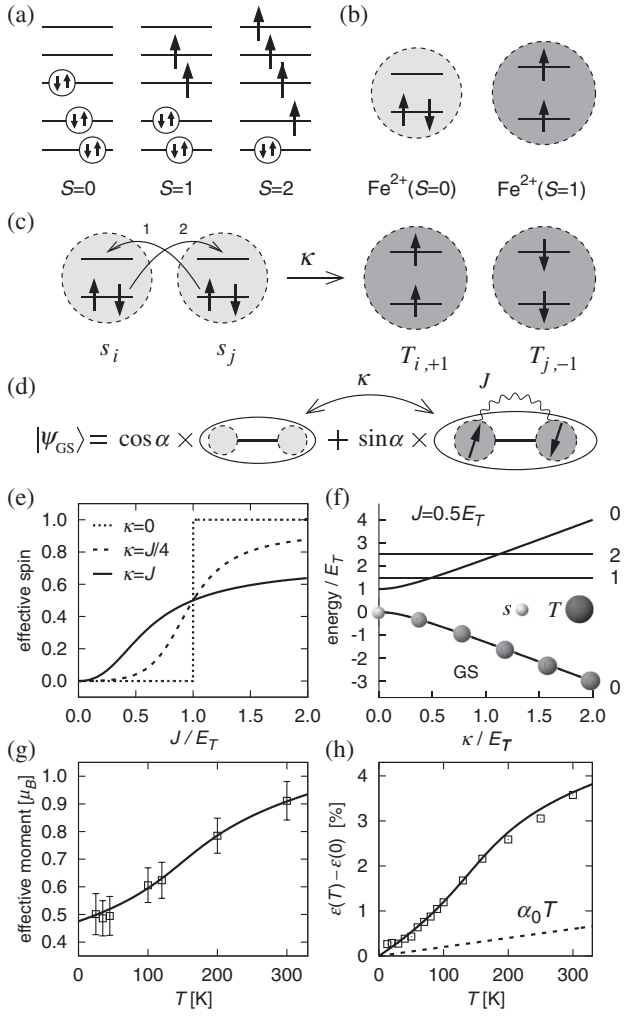

FIG. 1. (a) Schematic view of low ($S = 0$), intermediate ($S = 1$), and high ($S = 2$) spin states of $Fe^{2+}(3d^6)$. (b) $S = 0$ and $S = 1$ states differ in two electrons (out of six) occupying either the same or two different t_{2g} orbitals. The $S = 1$ state has a larger ionic radius. (c) The κ process generating a singlet pair of $S = 1$ triplets T of two Fe^{2+} ions, both originally in the $S = 0$ state (denoted by s). (d) The GS wave function of a Fe^{2+}-Fe^{2+} pair is a coherent superposition of two total-singlet states. (e) Effective spin (average occupation of $S = 1$ state) depending on the ratio of the coupling J between $S = 1$ states and their energy E_T. (f) Energy levels labeled by the total spin value of the Fe^{2+}-Fe^{2+} pair. Only singlet pairs are affected by κ. With increasing κ, the $S = 1$ states are gradually mixed into the GS. (g) Temperature dependence of the local magnetic moment $2n_T$, and (h) the c axis thermal expansion. Squares in (g,h) represent experimental data on $Ca_{0.78}La_{0.22}Fe_2As_2$ [28]. Dashed line in (h) is a thermal expansion excluding magnetoelastic term.

bonding. Basically, κ is a part of usual exchange process when local Hilbert space includes different spin states $S = 0,1$; hence, $\kappa \sim J$. Coupling J between $S = 1$ triplets is contributed also by their indirect interaction via the electron-hole Stoner continuum and, as expected, it reduces with doping [31] as the electron-hole balance of a parent semimetal becomes no longer perfect.

The Hamiltonian describing the above physics comprises the following three terms: on-site energy E_T of $S = 1$ triplet T relative to $S = 0$ singlet s, and the bond interactions κ, J,

$$\mathcal{H} = E_T \sum_i n_{T_i} + \sum_{\langle ij \rangle} [-\kappa_{ij}(D_{ij}^\dagger s_i s_j + \text{H.c.}) + J_{ij} \boldsymbol{S}_i \cdot \boldsymbol{S}_j]. \quad (1)$$

The operator $D_{ij}^\dagger$ creates a singlet pair of spin-full T particles on bond $\langle ij \rangle$. For a general spin S of T particles, $D_{ij} = \sum_M (-1)^{M+S} T_{i,+M} T_{j,-M}$ with $M = -S, \ldots, S$ denoting the $N = 2S + 1$ projections; physically, $N = 3$. The constraint $n_{si} + n_{Ti} = 1$ is implied [32,33].

The above model rests on three specific features of Fe pnictides or chalcogenides: (i) spin-state flexibility of Fe^{2+} that can be tuned by pressure increasing E_T, (ii) edge-sharing FeX_4 tetrahedral structure allowing "spin-mixing" κ term, and (iii) semimetallic nature which makes J values to decrease upon doping [31].

Figures 1(d)–1(f) demonstrate the behavior of spin-1 T particles ($N = 3$) on a single bond. The GS wave function $|\psi_{GS}\rangle = \cos\alpha|A\rangle + \sin\alpha|B\rangle$ is a superposition of two singlets $A = s_1^\dagger s_2^\dagger$ and $B = -(1/\sqrt{3}) \sum_M (-1)^M T_{1,M}^\dagger T_{2,-M}^\dagger$, with the "spin-mixing" angle $\tan 2\alpha = \sqrt{3}\kappa/(E_T - J)$. The GS energy $E_{GS} = (E_T - J) - \sqrt{(E_T - J)^2 + 3\kappa^2}$. At $\kappa = 0$, there is a sudden jump [Fig. 1(e)] from $S = 0$ state to $S = 1$ once the J-energy compensates the cost of having two T particles. At finite κ, the dynamical mixing of spin states converts this transition into a spin-crossover, where the effective spin-length $S_{eff} = n_T = \sin^2\alpha$ increases gradually. Figure 1(f) shows that κ term strongly stabilizes the singlet pair of T particles; this leads (see later) to a large biquadratic coupling $(\boldsymbol{S}_1 \cdot \boldsymbol{S}_2)^2$ which is essential in Fe pnictides [31,34,35].

We are ready to show the model in action, explaining recent observation of an unusual increase of the local moment upon warming [28]. This fact is at odds with Heisenberg and SDW pictures but easy to understand within the spin-crossover model. Indeed, the spin-length S_{eff} may vary as a function of E_T which, in turn, is sensitive to lattice expansion; in fact, Gretarsson *et al.* found that the moment value follows c-axis thermal expansion $\epsilon = \delta c/c$. We add (magnetoelastic) coupling $-A\epsilon n_T$ in Eq. (1), affecting E_T value, and evaluate ϵ and $\langle n_T \rangle_\epsilon$ self-consistently. This is done by minimizing the elastic energy $(1/2)K\epsilon^2 - K\alpha_0 T\epsilon + (1/4)Q\epsilon^4$ (α_0 is the usual thermal expansion coefficient), together with the GS energy E_{GS} given above. This results in a linear relation $\epsilon \simeq \alpha_0 T + (A/K)\langle n_T \rangle_\epsilon$ between the magnetic moment ($= 2n_T$) and lattice expansion. They both strongly increase with temperature if lattice is "soft" enough (i.e., small K), as demonstrated in Figs. 1(g) and 1(h) by employing

the parameters $E_T - J = 160$ meV, $\kappa = 60$ meV, $A = 1.5$ eV, $K = 4.55$ eV, $Q = 250$ eV, and $\alpha_0 = 0.2 \times 10^{-4}$ K^{-1}, providing a good fit to the experimental data of Ref. [28].

Turning to collective behavior of the model, we notice first that for $N \to \infty$ and large κ, the GS is dominated by tightly bound singlet dimers derived from the single-bond solution. The resonance of dimers on square-lattice plaquettes then supports a columnar state [36] breaking lattice symmetry without magnetic LRO [33]. In the opposite limit of $N = 1$, the model shows a condensation of T bosons. We found that the $N = 3$ model relevant here is also unstable towards a condensation of T particles with $S = 1$. This condensate hosts interesting properties not present in a conventional Heisenberg model. We discuss them based on the following wave function describing Gutzwiller-projected condensate of spin-1 T bosons:

$$|\Psi\rangle = \prod_i \left[\sqrt{1-\rho}\, s_i^\dagger + \sqrt{\rho} \sum_{\alpha=x,y,z} d_{\alpha i}^* T_{\alpha i}^\dagger\right]|\text{vac}\rangle, \quad (2)$$

where $\rho \in [0, 1]$ is the condensate density to be understood as the effective spin-length S_{eff}. The complex unit vectors $\boldsymbol{d}_i = \boldsymbol{u}_i + i\boldsymbol{v}_i$ ($u_i^2 + v_i^2 = 1$) determine the spin structure of the condensate in terms of the coherent states of spin-1 [37,38] corresponding to $T_x = (T_{+1} - T_{-1})/\sqrt{2}i$, $T_y = (T_{+1} + T_{-1})/\sqrt{2}$, $T_z = iT_0$. The GS phase diagram obtained by minimizing $\langle\Psi|\mathcal{H}|\Psi\rangle$ and cross-checked by an exact diagonalization on a small cluster is presented in Fig. 2. We have included nearest-neighbor (NN) and next-NN interactions and fixed their ratio at $J_2/J_1 = \kappa_2/\kappa_1 = 0.7$, reflecting large next-NN overlap via As ions. Like in $J_1 - J_2$ model, this ratio decides between (π, π) and $(\pi, 0)$ order. Figures 2(a) and 2(b) contain, apart from a disordered (uncondensed) phase ($\rho = 0$) at small κ, J, three distinct phases depending on κ/E_T and J/E_T values. (i) Ferroquadrupolar (FQ) phase with $\boldsymbol{u}_i = \boldsymbol{u}$ and $\boldsymbol{v}_i = 0$. This phase has zero magnetization and is characterized by the quadrupolar order parameter $\langle S^\alpha S^\beta - (1/3)S^2\delta_{\alpha\beta}\rangle = \rho((1/3)\delta_{\alpha\beta} - u_\alpha u_\beta)$ with $\boldsymbol{u}$ playing the role of the *director* [38]. This state, often referred to as "spin nematic," appears in biquadratic exchange [37–40] and optical lattice models [41–44]. (ii) Nonsaturated antiferromagnetic (ns-AF) phase with stripy magnetic order, specified by $\boldsymbol{u}_i = (0, 0, u)$ and $\boldsymbol{v}_i = (0, v, 0)e^{i\boldsymbol{Q}\cdot\boldsymbol{R}_i}$ with $\boldsymbol{Q} = (\pi, 0)$. The LRO moment $\langle\boldsymbol{S}\rangle$ given by $m = 2\rho uv$ can take values from 0 to $S_{\text{eff}} = \rho$. (iii) Saturated antiferromagnet (AF) with the same $\boldsymbol{Q}$ vector, but now with $u = v = 1/\sqrt{2}$ and $m = S_{\text{eff}} = 1$.

The part of the phase diagram relevant to pnictides is shown in Fig. 2(d). The decrease of J is associated with doping that changes the nesting conditions [31], while the increase of E_T is related to external or chemical pressure. Figures 2(e) and 2(f), shows that the LRO moment m quickly vanishes as J (E_T) values decrease (increase); however, the spin-length $S_{\text{eff}} = \rho$ remains almost constant

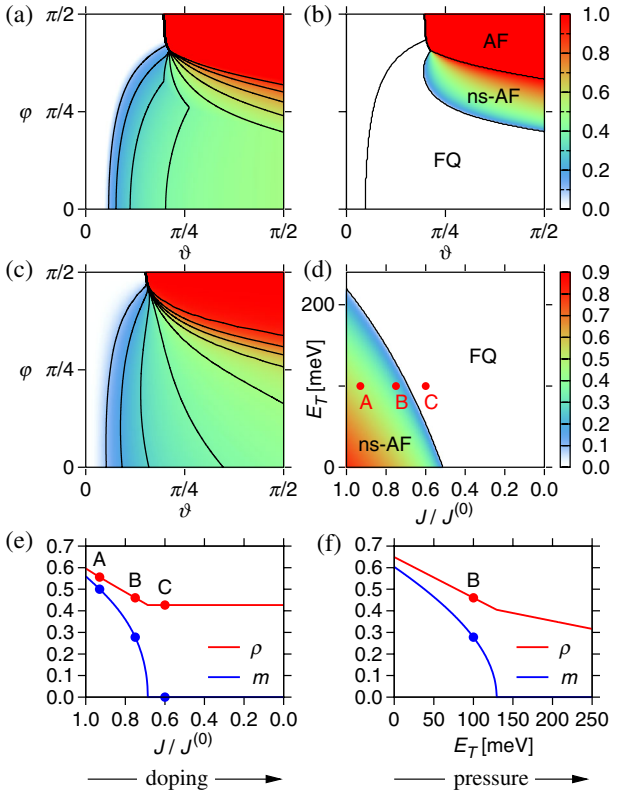

FIG. 2 (color online). (a) Condensate density $\rho(\equiv S_{\text{eff}})$ obtained from Eq. (2) as a function of angles ϑ, φ which parametrize the model (1) via $E_T = \cos\vartheta$, $\kappa_1 = \sin\vartheta\cos\varphi$, and $J_1 = \sin\vartheta\sin\varphi$. We set $\kappa_2/\kappa_1 = J_2/J_1 = 0.7$. (b) The ordered spin moment value m. (c) T occupation per site n_T obtained by an exact diagonalization of 12-site cluster, to be compared with ρ of panel (a). (d) The ordered moment m as a function of E_T and relative J-strength for fixed $\kappa_1 = 100$ meV, $\kappa_2 = 0.7\kappa_1$, $J_1^{(0)} = 140$ meV, $J_2^{(0)} = 0.7J_1^{(0)}$. (e,f) Effective spin length $\rho = S_{\text{eff}}$ and ordered moment m at the (e) $E_T = 100$ meV and (f) $J/J^{(0)} = 0.75$ lines through the phase diagram in (d).

($\sim 1/2$), corresponding to a fluctuating magnetic moment $\sim 1\mu_B$. This quantum state is driven by the κ process, which generates the spin-1 states in a form of singlet pairs.

We consider now the excitation spectrum. It is convenient to separate fast (density) and slow (spin) fluctuations. We introduce pseudospin $\tau = 1/2$ indicating the presence of a T particle, and a vector field $\boldsymbol{d}$ defining the spin-1 operator as $\boldsymbol{S} = -i(\boldsymbol{d}^\dagger \times \boldsymbol{d})$. The resulting Hamiltonian,

$$\mathcal{H} = E_T \sum_i \left(\frac{1}{2} - \tau_i^z\right) - \sum_{\langle ij\rangle} \kappa_{ij}(\tau_i^+ \tau_j^+ \boldsymbol{d}_i \cdot \boldsymbol{d}_j + \text{H.c.}) - \sum_{\langle ij\rangle} J_{ij}\left(\frac{1}{2} - \tau_i^z\right)\left(\frac{1}{2} - \tau_j^z\right)(\boldsymbol{d}_i^\dagger \times \boldsymbol{d}_i)\cdot(\boldsymbol{d}_j^\dagger \times \boldsymbol{d}_j) \quad (3)$$

is decoupled on a mean-field level. The condensate spin dynamics is then given by $O(3)$-symmetric Hamiltonian

$$\mathcal{H}_d = -\sum_{\langle ij\rangle} \tilde{\kappa}_{ij}(\boldsymbol{d}_i \cdot \boldsymbol{d}_j + \text{H.c.}) - \sum_{\langle ij\rangle} \tilde{J}_{ij}(\boldsymbol{d}_i^\dagger \times \boldsymbol{d}_i)\cdot(\boldsymbol{d}_j^\dagger \times \boldsymbol{d}_j) \tag{4}$$

with the renormalized $\tilde{\kappa}_{ij} = \kappa_{ij}\langle\tau_i^+\tau_j^+\rangle \approx \kappa_{ij}(1-\rho)\rho$ and $\tilde{J}_{ij} \approx J_{ij}\rho^2$. The excitations are found by introducing a, b, c bosons according to $\boldsymbol{d} = (d_x, d_y, d_z) = (a, ub - ive^{i\boldsymbol{Q}\cdot\boldsymbol{R}}c, -ive^{i\boldsymbol{Q}\cdot\boldsymbol{R}}b + uc)$ and replacing the condensed one as c, $c^\dagger \to \sqrt{1-n_a-n_b}$. The resulting ($a$, b) Hamiltonian is solved by the Bogoliubov transformation. A similar approach is used for the τ sector describing the condensate density fluctuations $\delta\rho = \delta S_{\text{eff}}$.

Shown in Fig. 3 is the excitation spectra for several points of the phase diagram. The spin-length fluctuations δS_{eff} are high in energy. Figure 3(b) focuses on the magnetic excitations. In the FQ phase, quadrupole and magnetic modes are degenerate and gapless at $\boldsymbol{q} = 0$. As the AF phase is approached, the gap at $\boldsymbol{Q}$ decreases and closes upon entering the magnetic phase. However, the higher energy magnons (which scale with S_{eff}) are not much affected by transition, apart from getting (softer) harder in a (dis)ordered phase; this explains the persistence of well-defined high-energy magnons into nonmagnetic phases [19,20].

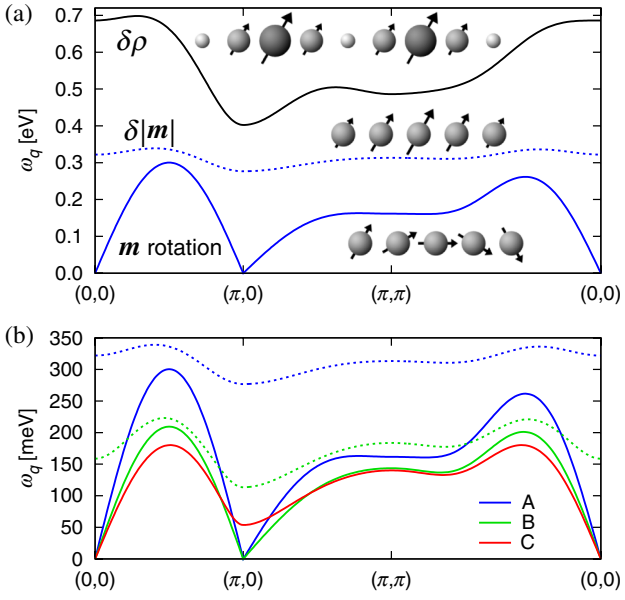

FIG. 3 (color online). (a) Dispersion of the condensate density ($\delta\rho$, solid-black) and the ordered moment-length ($\delta|\mathbf{m}|$, dotted-blue) fluctuations, and the magnon dispersion (solid-blue), at the point A in the phase diagram of Fig. 2(d). All three modes are active in resonant x-ray scattering, and the latter two in neutron scattering. (b) Evolution of the magnetic excitations going from FQ to the ns-AF phase [$C \to B \to A$ in Fig. 2(d)]. Twofold degenerate quadrupole waves (C) split into the magnon (solid lines) and the $\delta|\mathbf{m}|$ mode (dotted lines). The latter represents oscillations between the nematic and magnetic orderings and is gapful.

The magnetic modes in Fig. 3(b) resemble excitations of bilinear-biquadratic spin model [38]. In fact, the dispersion in FQ phase can be exactly reproduced [45] from an effective spin-1 model $\sum_{\langle ij\rangle}\tilde{J}_{ij}\boldsymbol{S}_i\cdot\boldsymbol{S}_j - \tilde{\kappa}_{ij}(\boldsymbol{S}_i\cdot\boldsymbol{S}_j)^2$, with $\tilde{J}$ and $\tilde{\kappa}$ given above. A large biquadratic coupling was indeed found to account for many observations in Fe pnictides [8,31,34]. We note, however, that this model possesses FQ and AF phases only and misses the ns-AF phase, where the ordered moment is reduced already at the classical level; also, it does not contain the key notion of the original model, i.e., formation of the effective spin S_{eff} and its fluctuations.

Singlet correlations inherent to the model may also lead to an increase of the paramagnetic susceptibility $\chi(T)$ with temperature [30]. Considering the nonmagnetic phase, we find that for the field parallel to the director $\boldsymbol{u}$, χ is temperature dependent, $\chi_\parallel = \frac{1}{2T}\int d\omega\,\mathcal{N}(\omega)\sinh^{-2}\frac{\omega}{2T}$, where $\mathcal{N}(\omega) = \sum_{\boldsymbol{q}}\delta(\omega - \omega_{\boldsymbol{q}})$ is the density of states (DOS) of magnetic excitations, while $\chi_\perp$ is constant. The average $\chi = (\chi_\parallel + 2\chi_\perp)/3$ (with additional factor of $4\rho^2\mu_B^2 N_A$) gives the measured $\chi(T)$, assuming slow rotations of the director. The DOS shown in Fig. 4(a) is contributed mainly by the regions around $(\pi, 0)$ and $(0, \pi)$ hosting AF correlations. The corresponding thermal excitations lead to the increase of χ [Fig. 4(b)].

To conclude, we proposed the model describing quantum magnetism of Fe pnictides. Their universal magnetic spectra, wide-range variations of the LRO moments, and emergent biquadratic-spin couplings are explained. The model stands also on its own: extending the Heisenberg models to the case of "mixed-spin" ions, it represents a novel many-body problem. Of particular interest is the effect of band fermions, which should have a strong impact on low-energy dynamics of the model, e.g., converting the $\boldsymbol{q} = 0$ Goldstone modes into overdamped spin-nematic fluctuations. Understanding the effects of coupling between local moments and band fermions, including

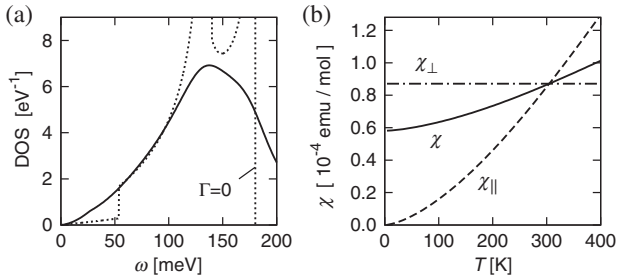

FIG. 4. (a) Density of states of the magnetic excitations calculated for the point C of Fig. 2(d). We included the damping (e.g., due to coupling to the Stoner continuum) in a form $\Gamma(\omega) = \min(\omega, \Gamma)$ with $\Gamma = \omega_Q/2$. The result with $\Gamma = 0$ is shown for comparison. (b) Temperature dependence of the uniform susceptibility χ. The components $\chi_\parallel$ ($\chi_\perp$) parallel (perpendicular) to the local director $\boldsymbol{u}$ are also shown.

implications for SC, should be the next step towards a complete theory of Fe pnictides.

J. C. acknowledges support by the Alexander von Humboldt Foundation, ERDF under project CEITEC (CZ.1.05/1.1.00/02.0068) and EC 7th Framework Programme (286154/SYLICA).

[1] Y. Kamihara, T. Watanabe, M. Hirano, and H. Hosono, J. Am. Chem. Soc. **130**, 3296 (2008).
[2] For a review of the experimental data, see, e.g., D. C. Johnston, Adv. Phys. **59**, 803 (2010).
[3] T. Yildirim, Physica (Amsterdam) **469C**, 425 (2009).
[4] C. Xu, M. Müller, and S. Sachdev, Phys. Rev. B **78**, 020501(R) (2008).
[5] Q. Si and E. Abrahams, Phys. Rev. Lett. **101**, 076401 (2008).
[6] C. Fang, H. Yao, W. F. Tsai, J. P. Hu, and S. A. Kivelson, Phys. Rev. B **77**, 224509 (2008).
[7] G. Uhrig, M. Holt, J. Oitmaa, O. P. Sushkov, and R. R. P. Singh, Phys. Rev. B **79**, 092416 (2009).
[8] D. Stanek, O. P. Sushkov, and G. S. Uhrig, Phys. Rev. B **84**, 064505 (2011).
[9] I. I. Mazin, D. J. Singh, M. D. Johannes, and M. H. Du, Phys. Rev. Lett. **101**, 057003 (2008).
[10] K. Kuroki, S. Onari, R. Arita, H. Usui, Y. Tanaka, H. Kontani, and H. Aoki, Phys. Rev. Lett. **101**, 087004 (2008).
[11] A. V. Chubukov, D. V. Efremov, and I. Eremin, Phys. Rev. B **78**, 134512 (2008).
[12] S. Graser, T. A. Maier, P. J. Hirschfeld, and D. J. Scalapino, New J. Phys. **11**, 025016 (2009).
[13] E. Kaneshita, T. Morinari, and T. Tohyama, Phys. Rev. Lett. **103**, 247202 (2009).
[14] H. Gretarsson *et al.*, Phys. Rev. B **84**, 100509(R) (2011).
[15] P. Vilmercati *et al.*, Phys. Rev. B **85**, 220503(R) (2012).
[16] M. D. Johannes, I. I. Mazin, and D. S. Parker, Phys. Rev. B **82**, 024527 (2010).
[17] I. I. Mazin and M. D. Johannes, Nat. Phys. **5**, 141 (2009).
[18] D. Reznik *et al.*, Phys. Rev. B **80**, 214534 (2009).
[19] M. Liu *et al.*, Nat. Phys. **8**, 376 (2012).
[20] K.-J. Zhou *et al.*, Nat. Commun. **4**, 1470 (2013).
[21] M. Wang *et al.*, arXiv:1303.7339.
[22] Z. P. Yin, K. Haule, and G. Kotliar, Nat. Mater. **10**, 932 (2011).
[23] J. Dai, Q. Si, J.-X. Zhu, and E. Abrahams, Proc. Natl. Acad. Sci. U.S.A. **106**, 4118 (2009).
[24] S.-P. Kou, T. Li, and Z.-Y. Weng, Europhys. Lett. **88**, 17010 (2009).
[25] W. Lv, F. Krüger, and P. Phillips, Phys. Rev. B **82**, 045125 (2010).
[26] *Spin Crossover in Transition Metal Compounds I*, edited by P. Gütlich and H. A. Goodwin (Springer, Berlin, 2004).
[27] S. Stackhouse, Nat. Geosci. **1**, 648 (2008).
[28] H. Gretarsson, S. R. Saha, T. Drye, J. Paglione, J. Kim, D. Casa, T. Gog, W. Wu, S. R. Julian, and Y.-J. Kim, Phys. Rev. Lett. **110**, 047003 (2013).
[29] J. T. Park *et al.*, Phys. Rev. B **86**, 024437 (2012).
[30] R. Klingeler *et al.*, Phys. Rev. B **81**, 024506 (2010).
[31] A. N. Yaresko, G.-Q. Liu, V. N. Antonov, and O. K. Andersen, Phys. Rev. B **79**, 144421 (2009).
[32] See Supplemental Material at http://link.aps.org/supplemental/10.1103/PhysRevLett.110.207205 for derivation of the Hamiltonian (1) from a two-orbital Hubbard model.
[33] To address a tetra/ortho structural (''orbital order'') transition, we may include also xz/yz orbital degeneracy of $S = 1$ triplets; this is left for future work.
[34] A. L. Wysocki, K. D. Belashchenko, and V. P. Antropov, Nat. Phys. **7**, 485 (2011).
[35] R. Yu, Z. Wang, P. Goswami, A. H. Nevidomskyy, Q. Si, and E. Abrahams, Phys. Rev. B **86**, 085148 (2012).
[36] N. Read and S. Sachdev, Phys. Rev. Lett. **62**, 1694 (1989).
[37] B. A. Ivanov and A. K. Kolezhuk, Phys. Rev. B **68**, 052401 (2003).
[38] A. Läuchli, F. Mila, and K. Penc, Phys. Rev. Lett. **97**, 087205 (2006).
[39] H. Tsunetsugu and M. Arikawa, J. Phys. Soc. Jpn. **75**, 083701 (2006).
[40] K. Harada and N. Kawashima, Phys. Rev. B **65**, 052403 (2002).
[41] E. Demler and F. Zhou, Phys. Rev. Lett. **88**, 163001 (2002); A. Imambekov, M. Lukin, and E. Demler, Phys. Rev. A **68**, 063602 (2003).
[42] S. K. Yip, Phys. Rev. Lett. **90**, 250402 (2003).
[43] C. M. Puetter, M. J. Lawler, and H.-Y. Kee, Phys. Rev. B **78**, 165121 (2008).
[44] M. Serbyn, T. Senthil, and P. A. Lee, Phys. Rev. B **84**, 180403(R) (2011).
[45] This can be understood using the identity $(\boldsymbol{S}_i \cdot \boldsymbol{S}_j)^2 = |\boldsymbol{d}_i \cdot \boldsymbol{d}_j|^2 + 1$. If $v \ll u \approx 1$, like in the FQ phase or close to it in the ns-AF phase, we recover the κ term of Eq. (4), $(\boldsymbol{S}_i \cdot \boldsymbol{S}_j)^2 \approx \boldsymbol{d}_i \cdot \boldsymbol{d}_j + \boldsymbol{d}_i^\dagger \cdot \boldsymbol{d}_j^\dagger$.